「Macromolecular Research」목차

정기간행영문지_ 28권 10호 · 2020년 9월

COVER PAPER

Curing Behavior of 4,4'-Diglycidyloxybiphenyl with *p*-Phenylene Diamine Derivatives

Arinola Isa Olamilekan and Hyeonuk Yeo*

Vol. 28, No. 10, pp 960-967 (2020) | SEP 25, 2020 | DOI 10.1007/s13233-020-8127-8

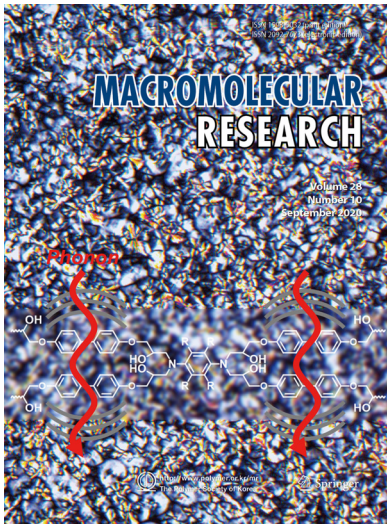

The curing behaviors of 4,4'-diglycidyloxybiphenyl (BP), the simplest liquid crystalline epoxy resin (LCER), with para-phenylene diamine derivatives investigated. The larger steric hindrance of the curing agents made nucleophilic curing rate slow and self-catalytic reaction less dominant. Based on the characteristics of LCER, the cured materials showed high heat resistance and thermal conductivity.

COMMUNICATION

Site-Selective Functionalization of Polydopamine Films *via* Aryl Azide-Based Photochemical Reaction

Jaehoon Jeong, Eunseok Kim, Wonwoo Jeong, Hyeongeun Kang, and Daewha Hong*

Macromol. Res., **28**, 885 (2020)

Site-selective conjugation method to functionalize polydopamine (pD) films is reported. Photo-irradiation of aryl azide group generated reactive nitrene groups that functionalize hydrocarbon networks of pD films, and combination of photomask allowed to immobilize initiator on predetermined region. A subsequent surface-initiated polymerization on their substrates produced a patterned polymer brush, expressing their own functionality on the surface platform.

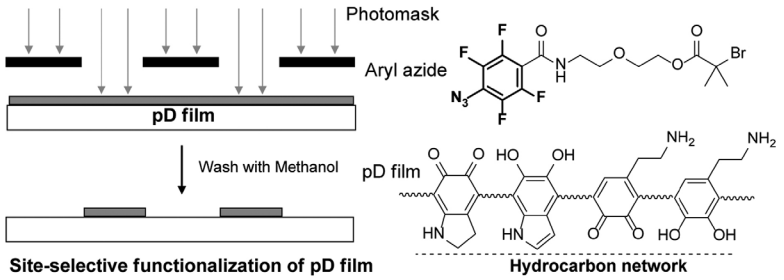

ARTICLES

Reticulated Vitreous Carbon Foams from Sucrose: Promising Materials for Bone Tissue Engineering Applications

Natalia Terán Acuña*,
Viviana Güiza-Argüello*,
and Elcy Córdoba-Tuta*

Macromol. Res., **28**, 888 (2020)

Polyurethane and cellulose foams were impregnated with a sucrose-based resin. To ensure homogeneous coverage of the foam surface, the excess resin was removed by extrusion using a roller mill. The impregnated sacrificial foams were then cured at 250 °C for 1 h with a heating rate of 1 °C/min and later carbonized in a tubular oven under inert atmosphere (N_2, 20 mL/min) at 900 °C for 1 h. The resulting reticulated vitreous carbon (RVC) foams showed favorable cytocompatibility and the ability to support human osteoblast adhesion.

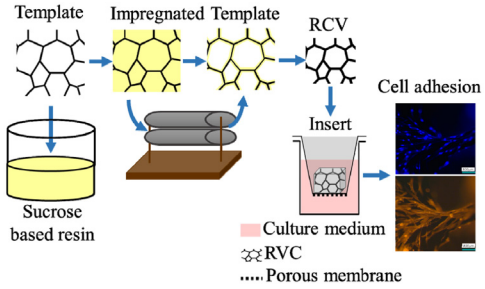

Synthesis of UV Curable, Highly Stretchable, Transparent Poly(urethane-acrylate) Elastomer and Applications Toward Next Generation Technology

Seohyun Kim, Juheon Lee,
and Haksoo Han*

Macromol. Res., **28**, 896 (2020)

Intermolecular hydrogen bonds form between urethane groups. Hydrogen bonds could break upon external stress and regenerate when stress is removed. Introducing butyl acrylate, large volume of side chain weakened the inter-chain interaction of polymer backbones and enlarged the polymer side chain bulkiness, as a results the elastomer showed low stress-strain values with high butyl acrylate ratios.

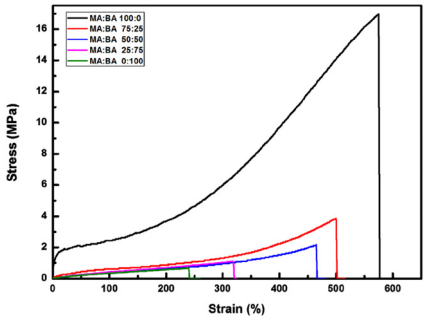

Synthesis and Characterization of Benzotriazole-Based Polymer Donors with Good Planarity for Organic Photovoltaics

Suha Lee, Jong-Woon Ha,
Hea Jung Park,
and Do-Hoon Hwang*

Macromol. Res., **28**, 903 (2020)

Two benzotriazole-based polymer donors, poly[4-(5-(2,5-bis((2-hexyldecyl)oxy)-4-(thiophene-2-yl)-phenyl)thiophene-2-yl)-5,6-difluoro-2-octyl-2*H*-benzo[*d*][1,2,3]triazole] (PPBTA-2HD) and poly[4-(5-(2,5-bis((2-hexyltridecyl)oxy)-4-(thiophene-2-yl)-phenyl)thiophene-2-yl)-5,6-difluoro-2-octyl-2*H*-benzo[*d*][1,2,3]triazole] (PPBTA-5HD), were synthesized, and their physical, optical, and electrochemical properties were characterized. PPBTA-2HD and PPBTA-5HD were used as electron donors and [6,6]-phenyl-C_{71}-butyric acid methyl ester ($PC_{71}BM$) as an electron acceptor in the active layer of the bulk-heterojunction solar cells. PPBTA-5HD exhibited better device performance than PPBTA-2HD, with a power conversion efficiency of 2.82% and a short-circuit current of 6.52 mA/cm^2.

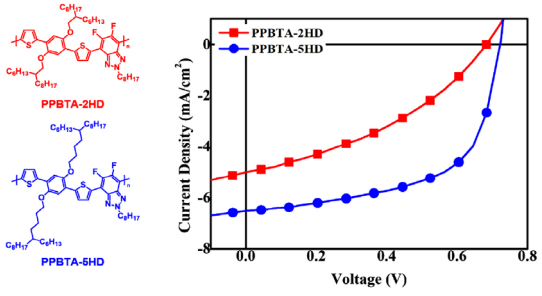

Syntheses and Properties of New Smectic Reactive Mesogens and Their Application in Guest-Host Polarizer

Yang Ye, Rui He, Eunche Oh, Shin-Woong Kang, Seung Hee Lee, Xiang-Dan Li, and Myong-Hoon Lee*

Macromol. Res., **28**, 910 (2020)

New smectic liquid crystalline monomers containing pyrimidine-based heteroaromatic ring and an acetylene linking group as a mesogenic core. Mixture of above monomers, dichroic dye and additives was injected into the sandwiched glass cell with rubbed alignment layers. Subsequent in-situ photopolymerization at room temperature successfully resulted in a thin film polarizer with good polarizing properties. The fabricated guest-host polarizer showed a dichroic ratio (DR) of 13.1 and a degree of polarization (DOP) of 95.5% with the thickness of 5 μm.

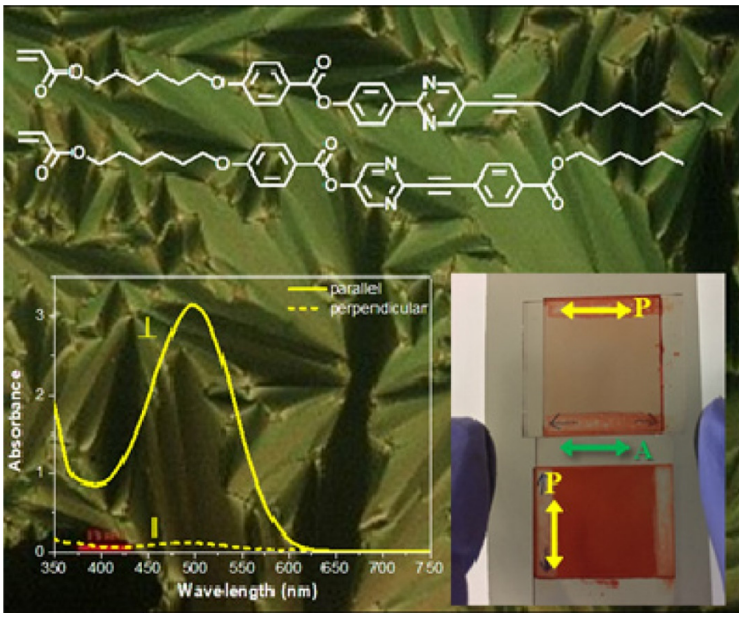

Synthesis and Opto-Electrical Properties of Novel Conjugated Small Molecule Bearing a B←N Moiety

Ka Yeon Ryu, Dan-Bi Sung, Yong-Ju Kwon, Hyun Yeong Kim, Chongmok Lee, Won-Suk Kim*, and Kyungkon Kim*

Macromol. Res., **28**, 919 (2020)

Effects of the B←N unit on the energy level of conjugated small molecule were investigated by synthesizing a new small molecule **BPDPP** (3,8-bis(5-(2,5-dioctyl-3,6-dioxo-4-(thiophen-2-yl)-2,3,5,6-tetrahydropyrrolo[3,4-c]pyrrol-1-yl)thiophen-2-yl)-6,6-dioctyl-6H-benzo[3,4][1,2]azaborolo[1,5-a]pyridin-5-ium-6-uide) *via* Suzuki coupling. For comparison, **CPDPP** (6,6'-(5,5'-(9,9-dioctyl-9H-fluorene-2,7-diyl)bis(thiophene-5,2-diyl))bis(2,5-dioctyl-3-(thiophen-2-yl)pyrrolo [3,4-c]pyrrole-1,4(2H,5H)-dione)) having the same chemical structure with **BPDPP** except the B←N unit is synthesized through the same coupling reaction. Absorption spectra and cyclovoltammetry analysis for these small molecules revealed that the B←N unit reduces the band gap of **BPDPP** by maintaining large oxidation potential. As a result, the blend film of **BPDPP** and $PC_{71}BM$ maintained 87.4% of the initial absorption intensity after 1sun light soaking test for 315 h. The photo stability of the **BPDPP** is significantly higher than the blend film of P3HT: $PC_{71}BM$, which maintained only 19.8% of the initial absorption intensity only after light soaking for 23 h.

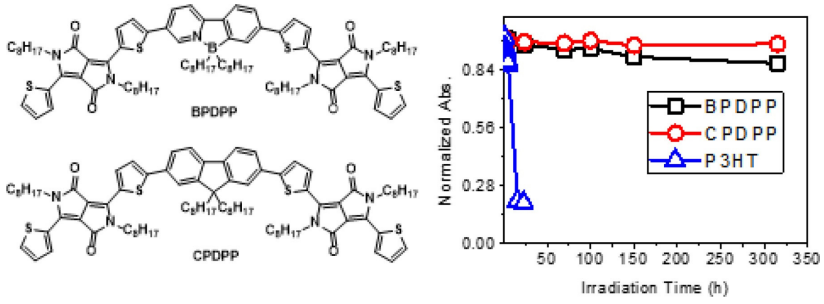

Effect of Electron Beam Irradiation on Gas-barrier Property of Biaxially Drawn Nylon/Montmorillonite Nanocomposite Films

Je Sung Youm, Jong-Jin Park, and Jeong Cheol Kim*

Macromol. Res., **28**, 925 (2020)

Nylon/MMT nanocomposite film was fabricated by the twin-screw extrusion, electron beam (EB) irradiation, and biaxial drawing. Irradiation induced the formation of a crosslinked network between the polymers and the organoclay in the composite film. The resultant film exhibited fine nanoclay dispersibility, significantly improved oxygen-gas barrier properties and tensile strength along with thermal shrinkage. These improvements are considered to be due to both EB irradiation and biaxial drawing.

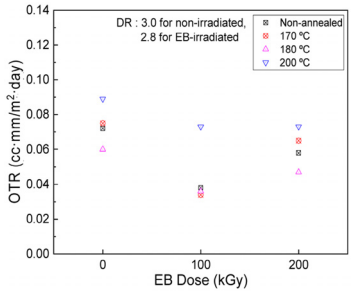

Study of Active Water Absorption of Polystyrene-Based Ionomers

In-Sub So and Joon-Seop Kim*

Macromol. Res., **28**, 932 (2020)

When the ion contents of the poly(styrene-co Na-methacrylate) (PSMANa) and poly(styrene-co Na-styrenesulfonate) (PSSNa) ionomers exceeded 6 and 10 mol%, respectively, the maximum amount of the water absorbed by the ionomers increased rapidly as the ion content increased, indicating the cluster-dominant ionomers exhibited stronger water absorption behavior. The small-angle X-ray scattering profiles also showed that the water uptake increased with increasing ion content of the ionomers, which was consistent with the results obtained by the swelling method.

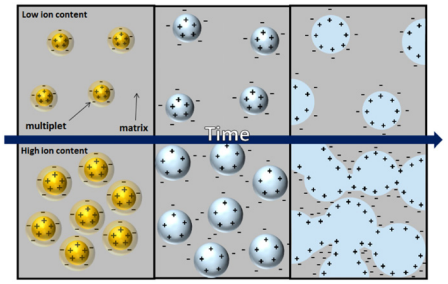

Effect of Multi-Level Microstructure on Local and Bulk Mechanical Properties in Micro-Injection Molded PC/PET Blend

Jianping Ren, Jing Jiang*, Zihui Li, Jianhua Hou, and Qian Li

Macromol. Res., **28**, 939 (2020)

Polycarbonate (PC), poly(ethylene terephthalate), and PC/PET microparts all exhibit typical "skin-core" morphologies. Photoacoustic Fourier transform infrared spectroscopy records reveal that the molecular chains orientation in the skin layer is more than 50% that in the core layer. The higher modulus in the shear layer is affected to a greater extent by high shear action in comparison with the frozen and core layers. SEM micrographs of the fracture sections demonstrated that different crack evolution patterns and fracture morphologies contributed to the difference in bulk mechanical performance.

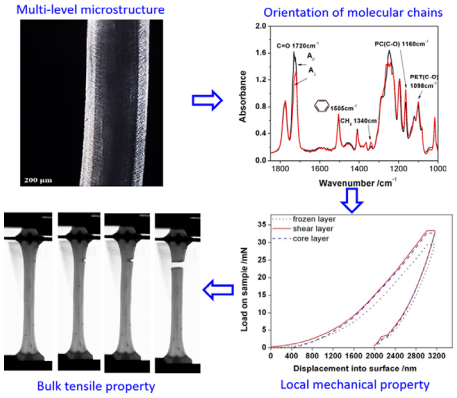

Facile Preparation of Polymer-Grafted Halloysite Nanotubes *via* a Redox System: A Novel Approach to Construct Antibacterial Hydrogel

Yanfang Ma, Zhihang Zhao, Boyan Tang, Yonggang Wu, and Hailei Zhang*

Macromol. Res., **28**, 948 (2020)

Commonly-used vinyl monomers were grafted on halloysite nanotubes (HNTs) in one step *via* a supernormal valence transition-metal-mediated redox system. Then a uniform hydrogel was constructed by mixing poly(triethyl(4-vinylbenzyl) phosphonium chloride-grafted HNTs with sodium polyacrylate-grafted HNTs, which show desirable antibacterial activity.

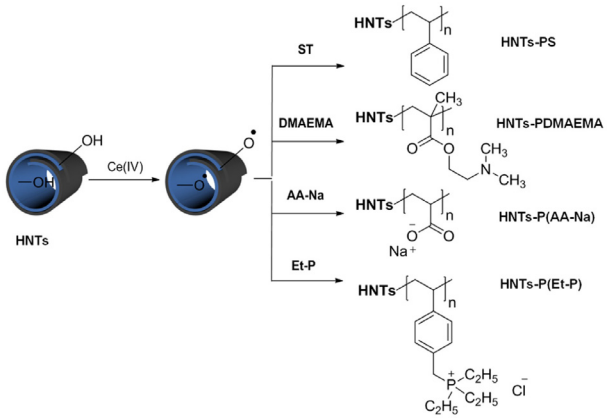

Interfacial Configurations of Lens-Shaped Particles

Kyu Hwan Choi, Tae Seok Seo, and Bum Jun Park*

Macromol. Res., **28**, 953 (2020)

Configuration behaviors of lens-shaped particles were studied by calculating the attachment energy and determining the energy minima. The interfacial pinning phenomena at the truncated or biconvex boundary and free-rotation of the particles were comprehensively investigated depending on wettability and geometric factors. This study can offer a simple design rule for the synthesis of anisotropic particles used as solid surfactants.

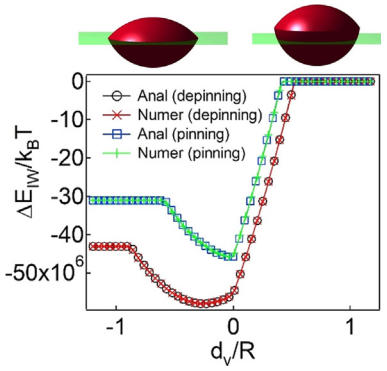

Curing Behavior of 4,4'-Diglycidyloxybiphenyl with *p*-Phenylene Diamine Derivatives

Arinola Isa Olamilekan and Hyeonuk Yeo*

Macromol. Res., **28**, 960 (2020)

Cover Paper

The curing factors such as the starting temperature, heat, and activation energy of 4,4'-diglycidyloxybiphenyl with *p*-phenylenediamine derivatives under various stereoscopic conditions were investigated. The steric hindrance induced a slower curing reaction and reduction in self-catalytic curing. In addition, cured materials showed high glass transition temperatures and thermal conductivities derived from the characteristics of the liquid crystal.

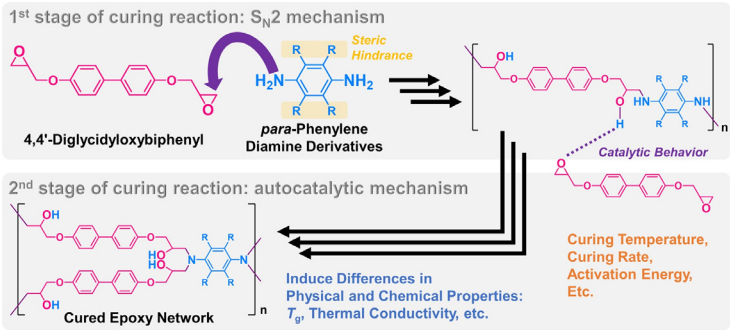

「Macromolecular Research」목차

정기간행영문지_ 28권 11호 · 2020년 10월

COVER PAPER

Nitrogen-Rich Magnetic Bio-Activated Carbon from Sericin: A Fast Removable and Easily Separable Superadsorbent for Anionic Dye Removal

Yeonkyung Hong, Hyoung-Joon Jin*, and Hyo Won Kwak*

Vol. 28, No. 11, pp 986-996 (2020) | OCT 25, 2020 | DOI 10.1007/s13233-020-8132-y

An eco-friendly porous activated carbon for anionic dye removal was prepared by utilizing sericin obtained from silkworm cocoons. Sericin-derived bio-activated carbon has a high surface area of 3289 m^2g^{-1}, and magnetic nanoparticles are introduced thereinto facilitate separation from contaminated water. The prepared sericin-derived hybrid carbon adsorbent achieved an excellent adsorption performance of 869.57 mg/g within a short time of 10 minutes. The results of this study suggest that sericin-derived activated carbon is a potential and effective adsorbent for rapidly removing dyes from aqueous solutions.

COMMUNICATION

Optimization of the Preparation and Characterization of Tannylated-Albumin Nanoagents

Yeong Jun Song, Sung Yun Jung,
Jin Hyuk Kim, and Kyeongsoon Park*

Macromol. Res., **28**, 969 (2020)

We optimized the preparation of tannylated-human serum albumin (TA-HSA) nanoagents including indocyanine green (ICG) and lobeglitazone (Lobe)-loaded complexes by simple mixing and characterized them. We set the optimal pH at 5 and the optimal weight ratio of [TA]/[HSA] at 1.5 when considering the redispersion of the prepared suspensions in PBS (pH 7.4) and incubation at 37 ℃ for the preparation of ICG and/or Lobe-loaded TA-HSA complexes. The immobilization of methoxy polyethylene glycol (mPEG) molecules on TA-HSA-ICG complexes significantly reduces the mean and Z-average sizes of these complexes from the microscale to the nanoscale. Moreover, the use of ICG increases the drug loading efficiency when preparing mPEG-TA-HSA-ICG/Lobe.

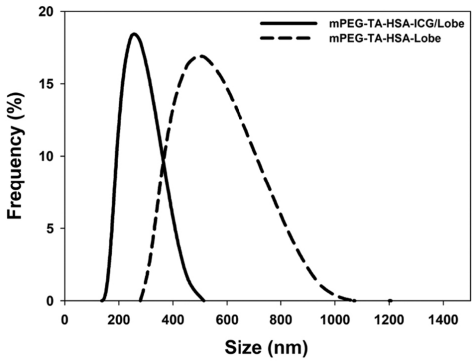

ARTICLES

Thermoelectric Properties of Polypyrrole Nanotubes

Yihan Wang, Qiang Yin*, Kai Du, Site Mo, and Qinjian Yin*

Macromol. Res., **28**, 973 (2020)

Using methyl orange (MO) as template, polypyrrole (PPy) nanotubes with different diameters have been successfully prepared. When the molar ratio of oxidant to pyrrole monomer was 1.5:1, PPy-1.5:1 nanotubes have smooth surface with diameter of 40-60 nm. The great degree of conjugation and the small conjugate defect of the molecular chains in PPy-1.5:1 contribute to electrical conductivity and Seebeck coefficient, resulting in the maximization of power factor of 0.55 $\mu Wm^{-1}K^{-2}$, about 22 orders of magnitude higher than PPy particles prepared under the same condition.

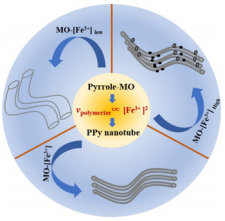

Evaluation of Hyaluronic Acid/Agarose Hydrogel for Cartilage Tissue Engineering Biomaterial

Joo Hee Choi, Jin Su Kim, Won Kyung Kim, Wonchan Lee, Namyeong Kim, Cheol Ui Song, Jun Jae Jung, Jeong Eun Song, and Gilson Khang*

Macromol. Res., **28**, 979 (2020)

Hyaluronic acid (HA) is one of the most applied biomaterials in a tissue engineering field due to its biocompatibility and its presence in the native extracellular matrix (ECM) of tissues. However, the mechanical property of the HA is weak and requires specific treatment to improve its properties. The application of Agarose (AG) hydrogel is widely studied and used as a support for the three-dimensional culture of cells due to its biocompatibility. Nevertheless, AG itself lacks the biological environment of the matrix which is unsuitable for the growth of the encapsulated cells. In this study, the composite of HA hydrogel and AG hydrogel (HA/AG hydrogel) is proposed to supplement the drawbacks of each hydrogel. HA provided enhanced microenvironment of matrix and AG improved the mechanical properties and assisted the cells. The characterization of the blended hydrogels was carried out with FT-IR, weight loss, swelling ratio, and compressive strength study. The biocompatibility and biological environment of the composite was evaluated by dimethylthiazol-2-yl-2,5-diphenyltetrazolium bromide; thiazolyl blue (MTT), live/dead staining, and morphological study. The composite biomaterial exhibited applicability for cartilage tissue engineering and the *in vitro* study of the cell-laden HA/AG hydrogel displayed potential for cartilage tissue engineering in the future.

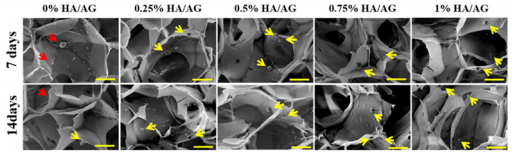

Nitrogen-Rich Magnetic Bio-Activated Carbon from Sericin: A Fast Removable and Easily Separable Superadsorbent for Anionic Dye Removal

Yeonkyung Hong, Hyoung-Joon Jin*, and Hyo Won Kwak*

Macromol. Res., **28**, 986 (2020)

Cover Paper

Sericin-derived activated carbon/magnetic nanoparticles (S-AC1.0/MNP) were prepared and used for adsorption of anionic dyes. S-AC1.0/MNP have a large specific surface area more than 2000 m^2/g and contains 2.4% nitrogen heteroatom. The prepared S-AC1.0/MNP adsorbents exhibited an excellent anionic methyl orange adsorption capacity of 870 mg/g due to the enhanced textural and chemical properties. Through this, it is expected that silk sericin has a great potential to be used as a precursor of carbon material, especially as a water restoration material.

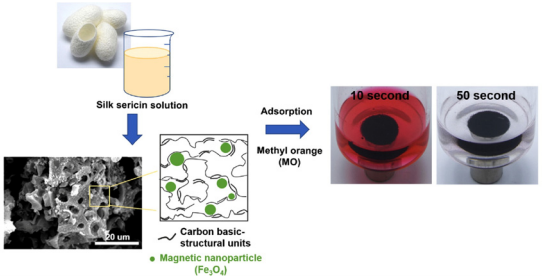

Effect of the Conformation Changes of Polyelectrolytes on Organic Thermoelectric Performances

Kyungwho Choi, Jihun Son, Yong Tae Park, Jung Sang Cho, and Chungyeon Cho*

Macromol. Res., **28**, 997 (2020)

Proper control of molecular conformation resulted in a significant improvement of thermoelectric behavior in PANi/MWNT-PAA nanocomposites through a combination of the efficient conjugate network and tightly packed nanostructure, which enhances the charge carrier mobility.

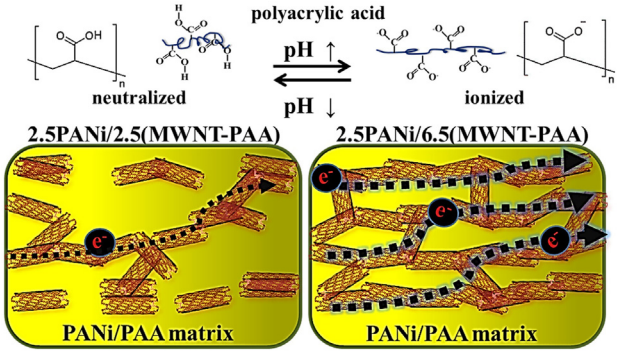

Dynamic Covalent Polymerization of Chalcogenide Hybrid Inorganic/Organic Polymer Resins with Norbornenyl Comonomers

Minho Kwon, Hongchan Lee, Seo-Hui Lee, Heung Bae Jeon, Min-Cheol Oh, Jeffrey Pyun*, and Hyun-jong Paik*

Macromol. Res., **28**, 1003 (2020)

We synthesized new chalcogenide hybrid inorganic/organic polymer (CHIPs) using inverse vulcanization with poly(Sulfur-*random*-Styrene) (p(S-*r*-Sty)) and new bifunctional norbornene comonomer. Bifunctional norbornene comonomers with different molecular architectures of thioester or disulfide linkage were synthesized and applied to the dynamic covalent bonding with p(S-*r*-Sty) for first time to prepare new functional organopolysulfide CHIPs.

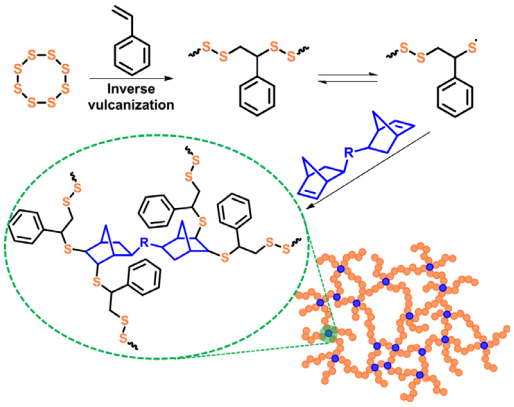

Poly(phenylene sulfide) Graphite Composites with Graphite Nanoplatelets as a Secondary Filler for Bipolar Plates in Fuel Cell Applications

Sang-Ha Kim, Jong Seok Woo, and Soo-Young Park*

Macromol. Res., **28**, 1010 (2020)

Graphite nanoplatelets (GNPs) have been used as a secondary filler to improve the electrical and thermal conductivities of poly(phenylene sulfide) (PPS)/graphite composites for use as bipolar plates in fuel cells. When 5 wt% GNP was added to the PPS/graphite composite, the in-plane electrical conductivity increased almost two-fold from 643 to 1340 $S \cdot cm^{-1}$, the through-plane electrical conductivity increased from 19 to 54 $S \cdot cm^{-1}$, the through-plane thermal conductivity increased approximately two-fold from 60 to 129 $W \cdot (mK)^{-1}$, and the flexural strength decreased slightly from 32 to 26 MPa.

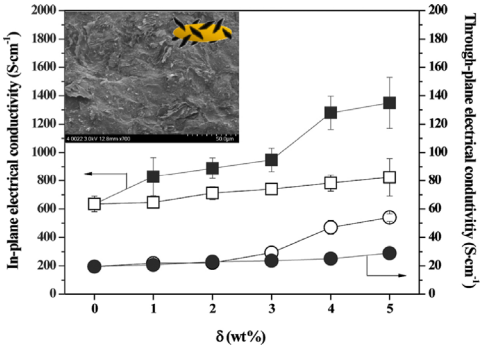

Injectable and Cryopreservable MSC-Loaded PLGA Microspheres for Recovery from Chemically Induced Liver Damage

Min-Jeong Park, Misook Choi, Mina Kim, and Don-Haeng Lee*

Macromol. Res., **28**, 1017 (2020)

Schematic of the injectable and cryopreservable mesenchymal stem cell (MSC)-loaded poly(D,L-lactic-*co*-glycolic acid) (PLGA) microspheres for the recovery from a chemically induced liver damage.

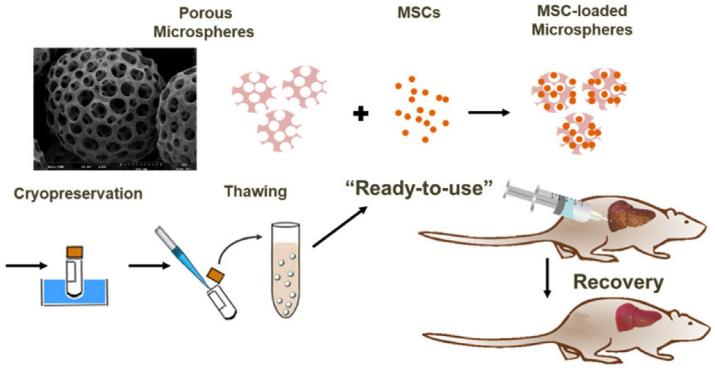

Nitroaromatic Compounds to Induce a Partial Positive Charge on the Silver Nanoparticle Surface for Facilitated Transport Membranes for Olefin/Paraffin Separation

Yebin Eum, Byung Su Kim, Il Seok Chae, Gi Hyeon Moon, Seul Chan Park, Jaeyoung Jang*, and Yong Soo Kang*

Macromol. Res., **28**, 1026 (2020)

Schematic illustration of silver nanoparticles (Ag NPs) positively charged by nitroaromatic compounds (NACs) and the mixed-gas selectivity of propylene over propane through composite membranes containing surface-activated Ag NPs dispersed in poly(*N*-vinyl pyrrolidone) (PVP) (Ag NPs/NAC composite membranes).

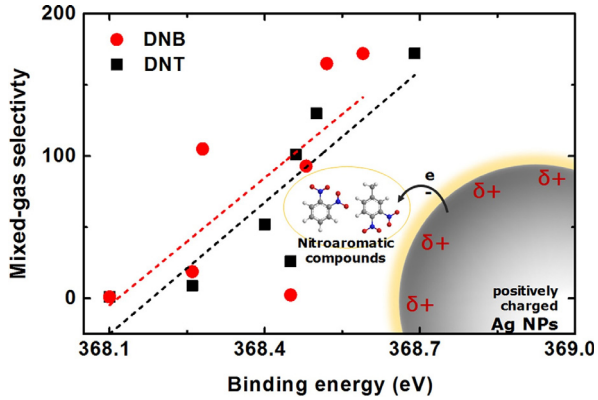

Effects of Polyether and Polyester Polyols on the Hydrophobicity and Surface Properties of Polyurethane/Polysiloxane Elastomers

Chang-An Xu, Mangeng Lu*, Kun Wu, and Jun Shi

Macromol. Res., **28**, 1032 (2020)

Polytetramethylene ether glycol (PTMG) has a more prominent effect on the surface hydrophobicity of polyurethane (PU)/polysiloxane than polycarbonate (PCDL) polyol of the same molecular weight. This is mainly related to the molecular structure of the polymer. The flexible chain of PTMG promotes the migration of silicone, and the surface of PTMGPU contains more silicone with low surface energy, thereby reducing the surface tension of PTMGPU, and as a result, the hydrophobicity is improved.

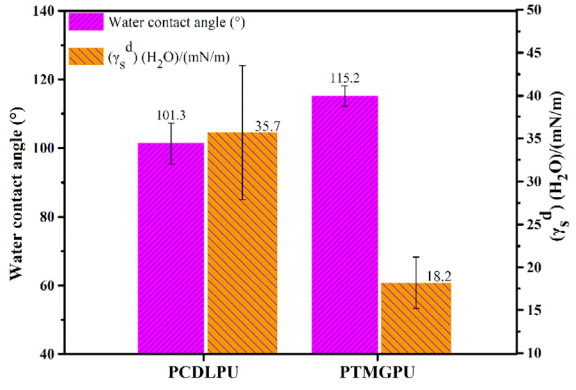

Silica/Epoxy Hybrid Encapsulation with High Heat-Resistance and Low Coefficient of Thermal Expansion

Sung Bum Lee, Ho Sik Lee, Chang Bum Son, Sung Hee Kim, and Jun Young Lee*

Macromol. Res., **28**, 1040 (2020)

Highly pure tri-functional triglycidyl p-aminophenol (TGPAP) epoxy with low viscosity was successfully synthesized by reacting epichlorohydrin with p-aminophenol using sodium hydroxide catalyst, followed by a physical thin film distillation process after synthesis. Silica/TGPAP hybrid was fabricated using TGPAP and two kinds of ground fumed silica with different size of 20 μm and 9 μm. Glass transition temperature of the hybrid was found to be as high as 185 °C and coefficient of thermal expansion was as low as 22.79 ppm/°C. From thermal shock test, no cracks were observed even after 1,000 cycles of thermal shock when 67% of silica was involved in the hybrid. In conclusion, silica/TGPAP hybrid encapsulation for electronic devices could be fabricated with high silica loading, resulting in improved processability, superior thermal shock resistance and low thermal expansion coefficient.

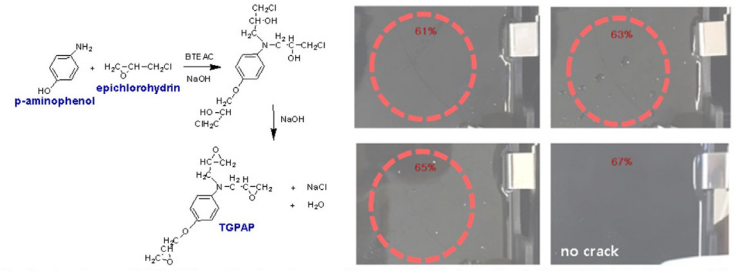

Synthesis scheme of triglycidyl p-aminophenol epoxy Thermal shock test results of silica/TGPAP hybrid encapsulation

In Situ Microfluidic Preparation and Solidification of Alginate Microgels

Samar Damiati*

Macromol. Res., **28**, 1046 (2020)

Despite the importance of alginate particles in synthetic bioarcheticture and drug delivery systems, synthesis of these particles suffers from several limitations. Thus, the current study presents various microfluidic models to generate alginate beads and investigate the influence of several parameters on their monodispersity. It is a simple user's guide to create alginate microgels in various architectures, including individual monodisperse or polydisperse beads, small clusters, and multicompartment systems.

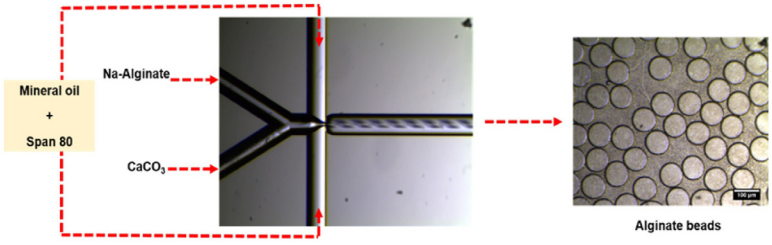

Alginate beads